Correlations of the Basicity of His 57 with Transition State Analogue Binding, Substrate Reactivity, and the Strength of the Low-Barrier Hydrogen Bond in Chymotrypsin†

Jing Lin, Constance S. Cassidy, and Perry A. Frey*

Institute for Enzyme Research, The Graduate School, and Department of Biochemistry, College of Agricultural and Life Sciences, University of Wisconsin—Madison, Madison, Wisconsin 53705

Received February 3, 1998; Revised Manuscript Received June 2, 1998

ABSTRACT: The basicity of His 57-N$^{\epsilon 2}$ within the low-barrier hydrogen-bonded (LBHB) diad His 57-Asp 102 and the ^{1}H NMR chemical shift of the LBHB proton in tetrahedral, hemiketal complexes of chymotrypsin with peptidyl trifluoromethyl ketones (peptidyl-TFKs) have been studied. The following results were obtained with various peptidyl-TFKs at 5 °C: *N*-Ac-Gly-DL-Phe-CF_3, pK_a = 11.1 and δ_{LBHB} = 18.7 ppm; *N*-Ac-L-Val-DL-Phe-CF_3, pK_a = 11.8 and δ_{LBHB} = 18.9 ppm; *N*-Ac-L-Leu-DL-Val-CF_3, pK_a = 10.3 and δ_{LBHB} = 18.9 ppm; and *N*-Ac-L-Leu-DL-naphthyl-CF_3, pK_a = 10.9 and δ_{LBHB} = 19.0 ppm. Results for peptidyl-TFKs with Phe in the P_1 position and *N*-Ac, *N*-Ac-Gly, *N*-Ac-L-Val, and *N*-Ac-L-Leu in the P_2 position were well correlated with literature values for inhibition constants K_i and k_{cat}/K_m for the corresponding peptidyl methyl esters. The plot of log K_i versus the apparent pK_a of His 57-N$^{\epsilon 2}$ displayed a slope of −0.77, and that of log k_{cat}/K_m for peptidyl methyl esters versus the pK_a of His 57-N$^{\epsilon 2}$ in corresponding peptidyl-TFK complexes gave a slope of 0.68. The slope of a plot of pK_a versus δ_{LBHB} was 3.7, and that of log k_{cat}/K_m for peptidyl methyl ester substrates versus δ_{LBHB} for the corresponding peptidyl-TFK−chymotrypsin complexes was 2.7. A plot of log K_i versus δ_{LBHB} displayed a slope of −3.0. These plots indicated that the pK_a of His 57 and substrate reactivity were correlated with increasing strength of the low-barrier hydrogen bond. The apparent pK_a of His 57-N$^{\epsilon 2}$ for the chymotrypsin−*N*-Ac-L-Leu-DL-Phe-CF_3 complex is 10.6 at 25 °C, whereas it is 12.0 at 5 °C [Cassidy, C. S., Lin, J. L., and Frey, P. A. (1997) *Biochemistry 36*, 4576−4584]. The apparent discrepancy is likely to be due to a temperature dependence in the cooperative ionization of His 57 in peptidyl-TFK complexes, which appears to be coupled to inhibitor dissociation, hydration and ionization of free peptidyl-TFK, ionization of Ile 16, and a conformational change.

Peptidyl-TFKs[1] form tetrahedral hemiketal complexes with chymotrypsin by nucleophilic addition of the 3-OH group of Ser 195 to their ketonic groups (*1*, *2*). These complexes are closely related to the tetrahedral intermediates or transition states in catalysis, and they incorporate a LBHB between His 57 and Asp 102 (*3*, *4*). Spectroscopic analyses of complexes formed with two peptidyl-TFKs as a function of pH have given values of 10.8−12.0 for the apparent pK_a for N$^{\epsilon 2}$ of histidine in the diad His 57-Asp 102 (*5*). It was concluded that the chemical shift for the LBHB and the apparent pK_a of the diad depended upon the structure of the peptidyl group. A new concept for the mechanism of catalysis by chymotrypsin was proposed, in which substrate-induced steric compression in the catalytic site brought about LBHB-facilitated general base catalysis. This mechanism accounted for the nucleophilic reactivity of Ser 195 and the stabilization of the tetrahedral intermediate by the LBHB (*4*, *5*).

The inhibition constants for peptidyl-TFKs decrease with increasing hydrophobicity of the amino acid in the second aminoacyl position P_2 (*2*).[2] Furthermore, decreasing inhibition constants for peptidyl-TFKs with phenylalanine at P_1

† This work was supported by Grant GM 51806, and C.S.C. was supported by Predoctoral Training Grant GM 08505 from the National Institute of General Medical Sciences. This study made use of the National Magnetic Resonance Facility at Madison, which is supported by NIH Grant RR02301 from the Biomedical Research Technology Program, National Center for Research Resources. Equipment in the facility was purchased with funds from the University of Wisconsin, the NSF Biological Instrumentation Program (Grant DMB-8415048), the NIH Biomedical Research Technology Program (Grant RR02301), the NIH Shared Instrumentation Program (Grant RR02781), and the U.S. Department of Agriculture.

[1] Abbreviations: *N*-Ac**LF**-CF_3, *N*-acetyl-L-leucyl-DL-phenylalanyl trifluoromethyl ketone; *N*-Ac**VF**-CF_3, *N*-acetyl-L-valyl-DL-phenylalanyl trifluoromethyl ketone; *N*-Ac**GF**-CF_3, *N*-acetylglycyl-DL-phenylalanyl trifluoromethyl ketone; *N*-Ac**LV**-CF_3, *N*-acetyl-L-leucyl-DL-valyl trifluoromethyl ketone; *N*-Ac-F-CF_3, *N*-acetyl-DL-phenylalanyl trifluoromethyl ketone; *N*-Ac**LNp**-CF_3, *N*-acetyl-L-leucyl-DL-naphthyl trifluoromethyl ketone; *N*-Ac**LV**-OCH_3, *N*-acetyl-L-leucyl-L-valyl methyl ester; peptidyl-TFK, peptidyl trifluoromethyl ketone; Boc**APV**B$(OH)_2$, butyloxycarbonyl-alanyl-prolyl-valine boronic acid; CHES, 2-(*N*-cyclohexylamino)ethanesulfonic acid; CAPS, 3-(cyclohexylamino)-1-propanesulfonic acid; DMSO, dimethyl sulfoxide; KP_i, potassium phosphate; TLC, thin-layer chromatography; LBHB, low-barrier hydrogen bond; δ_{LBHB}, NMR chemical shift of the low-barrier hydrogen-bonded proton in complexes of peptidyl-TFK with chymotrypsin.

[2] The site nomenclature adopted here is that of Kraut (*6*). When it is applied to peptidyl-TFKs, P_1, P_2, etc., are the aminoacyl residues in the peptidyl-TFKs reading from the carbonyl group to the N terminus, and S_1, S_2, etc., are the corresponding subsites of chymotrypsin occupied by residues P_1, P_2, etc., in the enzyme−inhibitor complexes.

S0006-2960(98)00278-5 CCC: $15.00
Published on Web 08/05/1998

and various aminoacyl groups at P_2 are correlated with increasing values of k_{cat}/K_m for the corresponding methyl esters reacting as substrates of chymotrypsin (*2*). Therefore, the reactivities of peptidyl methyl esters acting as substrates and the inhibitory potencies of peptidyl-TFKs acting as transition state analogue inhibitors for chymotrypsin are correlated and depend on the nature of the aminoacyl group in position P_2.

In this paper, we present the results of ^{1}H NMR analysis of a series of chymotrypsin−peptidyl-TFK complexes and report values of δ_{LBHB}, as well as apparent pK_as for $N^{\epsilon 2}$ of the His 57-Asp 102 diad in these complexes. Data on complexes of chymotrypsin with peptidyl-TFKs incorporating phenylalanine at P_1 but varying in P_2 show a positive correlation of δ_{LBHB} with the basicity of the diad, a positive correlation of the inhibitory efficacy with the basicity of the diad, and a positive correlation of the diad basicity with the reactivities of the corresponding peptidyl methyl esters as substrates. The results further support the mechanism of LBHB-facilitated general base catalysis that has been proposed for His 57 and Asp 102 in chymotrypsin (*4*, *5*).

EXPERIMENTAL PROCEDURES

Supplies. α-Chymotrypsin (type II, crystallized three times from bovine pancreas), *N*-acetyl-L-leucine, valyl methyl ester hydrochloride, and CHES were obtained from Sigma and were used without further purification. Peptidyl trifluoromethyl ketones other than *N*-Ac**LV**-CF_3 were synthesized as previously described (*1*). DMSO-d_6, acetonitrile-d_3, 99% D_2O, and CAPS were purchased from Aldrich. Other chemicals were purchased commercially and used as supplied.

Synthesis. 1,1,1-Trifluoro-3-(*N*-acetyl-L-leucylamido)-4-methyl-2-pentanol was synthesized by coupling 3-amino-4-methyl-1,1,1-trifluoro-2-pentanol hydrochloride salt (*7*) with *N*-acetyl-L-leucine by the previously described method (*1*). ^{1}H NMR (300 MHz, $CDCl_3$/10% DMSO-d_6): δ 0.87−0.99 (12H, m), 1.45−1.72 (3H, m), 1.99 (3H, m), 2.12−2.20 (1H, m), 3.92−4.03 (1H, m), 4.07−4.20 (1H, m), 4.49−4.57 (1H, m), 5.80 (1H, dd, J = 6, 15 Hz), 6.97−7.23 (2H, m). ^{13}C NMR (75.5 MHz, $CDCl_3$/10% DMSO): δ 69.30 (CH, q), 125.7 (C, q).

1,1,1-Trifluoro-3-(*N*-acetyl-L-leucylamido)-4-methyl-2-pentanone (*N*-Ac**LV**-CF_3) was obtained from the oxidation of 1,1,1-trifluoro-3-(*N*-acetyl-L-leucylamido)-4-methyl-2-pentanol with $KMnO_4$, as described in syntheses of other peptidyl-TFKs (*1*). ^{1}H NMR (300 MHz, acetone-d_6): δ 0.83−0.97 (12H, m), 1.45−1.74 (3H, m), 2.23−2.36 (1H, m), 4.13−4.75 (2H, m), 7.30−7.98 (N-H). ^{13}C NMR (75.5 MHz, acetone-d_6): δ first isomer 17.9 (CH_3), 19.9 (CH_3), 22.5 (CH_3), 23.0 (CH_3), 23.5 (CH_3), 25.5 (CH), 30.0 (CH), 42.0 (CH_2), 52.0 (CH), 60.1 (CH), 116.8 (C, q), 171.0 (C), 174.2 (C), 191.1 (C, q); δ second isomer 17.9 (CH_3), 20.0 (CH_3), 22.5 (CH_3), 23.0 (CH_3), 23.5 (CH_3), 25.7 (CH), 30.0 (CH), 42.1 (CH_2), 52.0 (CH), 60.2 (CH), 116.8 (C, q), 171.0 (C), 174.2 (C), 191.1 (C, q); hydrate form 95.5 (C, q). High-resolution MS: *m*/*e* 324.1676, $C_{14}H_{23}N_2O_3F_3$ requires 324.1661; 324 (M^+), 309, 268, 227, 128.

N-Acetyl-L-leucyl-L-valyl methyl ester was synthesized as follows. L-Valyl methyl ester was prepared by reaction of its hydrochloride salt with excess potassium carbonate and extraction of the free methyl ester into diethyl ether. *N*-Acetyl-L-leucyl-L-valyl methyl ester was then synthesized by the mixed anhydride method, coupling *N*-Ac-L-leucine with L-valyl methyl ester, by the procedure described in the Supporting Information of Brady et al. (*2*). The product was purified on a silica gel column with 4:1 chloroform/ethyl acetate as the solvent. Fractions containing the product were identified by TLC with phosphomolybdic acid as an indicator. The purity of the compound was verified by ^{1}H and ^{13}C NMR. The assignments of the peaks are based on the previous assignment of similar peptides containing leucine and valine (*2*). ^{1}H NMR (500 MHz, $CDCl_3$): δ 0.72−1.06 (12H, m, Leu and Val CH_3s), 1.37−1.85 (4H, m, Leu β-CH_2, Val β-CH, and Leu γ-CH), 1.9 (3H, s, acetyl CH_3), 3.7 (3H, s, methyl ester CH_3), 4.34−4.69 (2H, α-CHs of Leu and Val), 5.63−6.09 (1H, d, NH), 6.33−6.61 (1H, d, NH). ^{13}C NMR (125.7 MHz, decoupled, $CDCl_3$): δ 17.91, 19.13, 22.48, 23.01 (CH_3s), 41.25 (CH_2), 51.99, 57.44 (α-CHs), 24.94, 31.32 (CHs), 170.3, 172.3, 172.4 (carbonyls).

pH Titrations of Chymotrypsin−Peptidyl-TFK Complexes by ^{1}H NMR at 5 °C. Solutions of 1.8 mM chymotrypsin were prepared with peptidyl-TFKs at pHs ranging from 7 to 12.4 in 0.5 M buffers (CAPS, CHES, and phosphate). Peptidyl-TFKs were dissolved in acetonitrile or DMSO and added in microliter aliquots to the chymotrypsin samples so that the solutions contained 4% solvent and >3.6 mM peptidyl-TFK, as well as 0.04% w/v sodium 3-(trimethylsilyl)-1-propanesulfonate in D_2O as an internal standard. The pH of each sample was measured at 5 °C. The ratio of inhibitor to chymotrypsin was ≥3:1, adjusted to ensure that most of the chymotrypsin was present as the tetrahedral, hemiketal complex with the peptidyl-TFK.

^{1}H NMR spectra were acquired on a Bruker DMX 500 MHz spectrometer using a nonsaturating water signal suppression program at 5 °C (*8*). The probe was tuned for each sample and the 90° pulse calibrated. The water signal was suppressed using a 1-1 pulse sequence program. Spectral conditions were 8000 time domain points and 8000 scans, with a 0.7 s delay between acquisitions and a spectral width of 22 522 Hz.

The data were processed with a Silicon Graphics workstation using the Felix 95 software package. The exponential line broadening was set to 20 Hz. Baselines were corrected with a fifth- to seventh-order polynomial, and the low-field signals were integrated by cutting and weighing. The relative areas of the low-field peaks for complexes of peptidyl-TFK with chymotrypsin (18−19 ppm) and that for free chymotrypsin at 15 ppm (neutral His 57) were determined. In the cases of the slow-binding inhibitors, the enzyme was not fully saturated with the inhibitor under the experimental conditions; therefore, the relative peak areas were corrected for the uncomplexed enzyme at pH 8.5. Increasing the ratio of inhibitor to enzyme for several of the complexes, including *N*-Ac**F**-CF_3 and *N*-Ac**LF**-CF_3, did not change the relative areas of the low-field peaks. From the integrated areas of the signal for the peptidyl-TFK−chymotrypsin complex at 18−19 ppm and that for free chymotrypsin at 15 ppm, the fraction in the form of the peptidyl-TFK complex was calculated with I_{LBHB} = (area at 18−19 ppm)/[(area at 18−19 ppm) + (area at 15 ppm)]. I_{LBHB} is the fraction of total chymotrypsin in the form of the peptidyl-TFK−hemiketal adduct.

Table 1: Physicochemical Data for Interactions of Peptidyl-TFKs and Peptidyl Methyl Esters with Chymotrypsin

peptidyl-TFK	K_i (μM)[a]	δ_{LBHB} (ppm)[b]	pK_a^{app} (His 57-N$^{\epsilon 2}$)[c]	k_{cat}/K_m (M^{-1} s^{-1})[d] (methyl esters)
N-Ac**LF**-CF_3	1.2, 2.4	18.93	12.1	14.3×10^5
N-Ac**VF**-CF_3	2.8, 4.5	18.86	11.8	9.88×10^5
N-Ac**GF**-CF_3	18, 12	18.68	11.1	1.89×10^5
N-Ac**F**-CF_3	17, 30, 20, 40	18.61	10.7	1.81×10^5
N-Ac**LNp**-CF_3	0.87, 0.63, 1.1, 0.67	19.0	10.9	ND
N-Ac**LV**-CF_3	170	18.9	10.3	19

[a] Values reported in refs *1*−*3* except K_i for *N*-Ac**LV**-CF_3, which was measured in this work. [b] Chemical shifts for the low-field LBHB proton in the first four entries were measured at pH 8.5 with an average deviation of ±0.03 ppm in two independent determinations. Single values were obtained for the last two entries. [c] Values for pK_a^{app} were measured at 5 °C with an estimated error of ±0.2. Values for *N*-Ac**LF**-CF_3 and *N*-Ac**F**-CF_3 were reported previously as 12.0 and 10.8, respectively, and have been updated with additional measurements (*5*). [d] Values for the corresponding peptidyl methyl esters are from ref *2*, except for k_{cat}/K_m for *N*-Ac**LV**-OCH_3, which was measured in this work.

pH Titrations by ^{1}H NMR at 25 °C. The apparent pK_as of N$^{\epsilon 2}$ in His 57-Asp 102 of chymotrypsin complexed with *N*-Ac**LF**-CF_3 or *N*-Ac**LNp**-CF_3 at 5 °C were determined by the method described above at 25 °C with minor modifications. The concentration of inhibitor was 3 times that of chymotrypsin, and the spectra were obtained from pH 7 to 11.

*pH-Stat Kinetic Assay of N-Ac**LV**-OCH_3 as a Substrate.* The assay solution was contained in a 4 mL vial and stirred with a magnetic flea. The temperature was equilibrated by a water bath, and the starting volume of the assay was 2 mL. Because *N*-Ac**LV**-OCH_3 was found to be an extraordinarily poor substrate, the enzyme concentration was 4 μM and the substrate concentration was varied from 1.6 to 12 mM. The assay was repeated at least once with each concentration of the substrate. The buffer was 1 mM KP_i with 100 mM K_2SO_4 at pH 7.0. The substrate stock solution of 0.32 M was prepared in acetonitrile. A 0.2 mM chymotrypsin stock solution was prepared in buffer, and the pH was adjusted to 7.0 by addition of small aliquots of 0.1 M NaOH. The volume of organic solvent added to the assay was such that all samples contained less than 5% (v/v) organic solvent. The vial was flushed with nitrogen throughout the course of the reaction to prevent the effects of CO_2 gas on the pH measurements. The reaction was initiated by the addition of chymotrypsin, and the pH was maintained at 7 by the addition of aliquots of 1 mM NaOH every 30 s for the duration of the assay. The concentration of the product was calculated by determining the moles of NaOH added and dividing by the total volume of the solution at each time point. The slope of the plot of product versus time is the rate constant in units of molar per second. The values for multiple runs were averaged, and the data were computer fitted to the Michaelis−Menten equation, $v = VA/(K + A)$.

*Acid Ionization Constant of the N-Ac**LV**-CF_3 Hydrate.* The inhibitor was dissolved in DMSO, and a 25 μL aliquot was added to a solution containing 0.1 M NaCl in deionized, distilled water. Aliquots of standardized NaOH were added, and the pH of the solution was recorded every 2 min. As a control, a solution of 0.1 M NaCl in deionized, distilled water was titrated with NaOH and the data points were subtracted from the titration of the inhibitor. The plot of volume of NaOH versus pH was computer fitted to the equation $Y = A + B/(1 + H/K)$ to determine a pK_a value for the hydrate at 25 °C of 10.4. The experiment was modified and repeated at 5 °C with 0.5 M NaCl. We were unable to determine an accurate pK_a value at 5 °C due to the titration of NaOH at high pH, but a lower limit of 11 was established for the pK_a of the hydrate at this temperature.

*Inhibition of Chymotrypsin by N-Ac**LV**-CF_3.* The inhibition constant was measured by analyzing the effect of the inhibitor on the reaction progress curves for the hydrolysis of *N*-benzoyl-L-tyrosine ethyl ester. The progress curves were measured at 25 °C spectrophotometrically at pH 7.5 in 100 mM KP_i buffer at a chymotrypsin concentration of <1 nM, and the substrate was present at 0.02 M at inhibitor concentrations of 1.25, 1.50, and 2.00 μM. The K_i value of 170 μM was calculated from progress curves at each inhibitor concentration using the equation

$$K_i = v_s[I]/[(v_o - v_s)(1 + [S]/K_m)] \quad (1)$$

where v_s is the steady state rate after the onset of inhibition, v_o is the steady state rate in the absence of inhibitor, and K_m for *N*-benzoyl-L-tyrosine ethyl ester is 11.5 μM (*1*).

RESULTS AND DISCUSSION

Values of chemical shifts for the low-field protons bridging His 57 and Asp 102 in complexes of chymotrypsin with various peptidyl-TFKs having phenylalanine, naphthyl, or valine in the P_1 position and *N*-Ac, *N*-Ac-L-Leu, *N*-Ac-L-Val, or *N*-Ac-Gly in the P_2 position are given in Table 1. The apparent pK_a values for ionization from N$^{\epsilon 2}$ of the His 57-Asp 102 diad at 5 °C are also included, as well as the previously determined inhibition constants and the k_{cat}/K_m values for the corresponding peptidyl methyl ester substrates at 25 °C (*2*). The methyl ester substrates differ from the peptidyl-TFKs in the presence of the methoxyl leaving group which is in place of the trifluoromethyl group of the inhibitors.

Initial studies focused on the variation of the P_2 residue, which binds to the S_2 aminoacyl site of chymotrypsin, with phenylalanine in the P_1 position and binding to the S_1 specificity pocket. The value of δ_{LBHB} increased as the hydrophobicity of the P_2 residue increased. The downfield signal appeared at lower field and was narrower than that for the protonated diad in free chymotrypsin (*5*, *9*). At higher pHs, the decrease in the intensity of the low-field signal and the growth of a signal at 15 ppm indicated the ionization of the diad at N$^{\epsilon 2}$. The 15 ppm signal resulting from the ionization was indistinguishable in chemical shift and line width from that for the His 57-Asp 102 diad in free chymotrypsin at high pH (*5*).

The apparent pK_a values for N$^{\epsilon 2}$ of His 57 listed in Table 1 were obtained from the titration curves of signal intensity

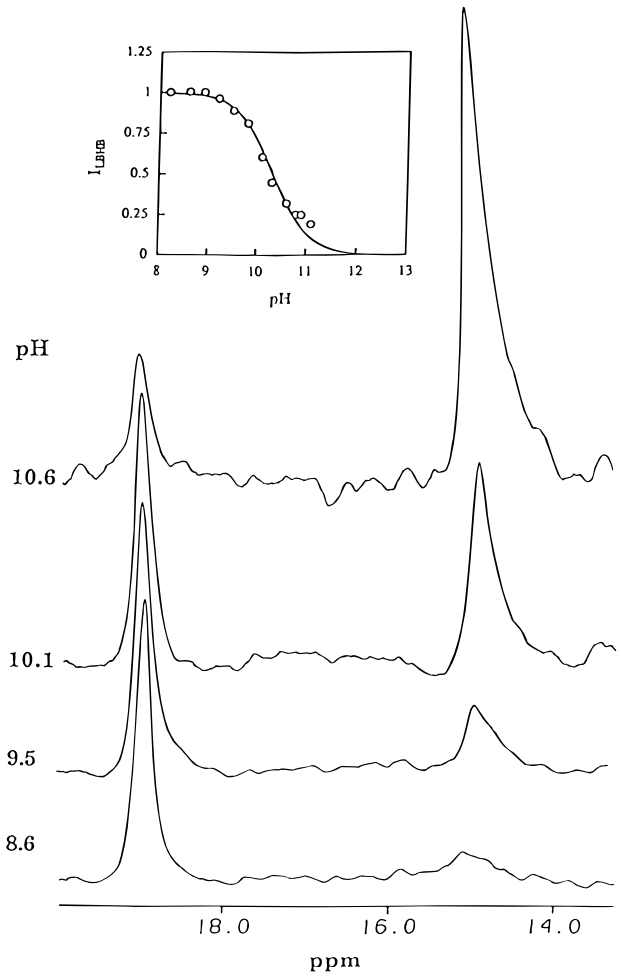

FIGURE 1: pH titration of the *N*-Ac**LV**-CF_3−chymotrypsin complex by ^{1}H NMR at 5 °C. The low-field ^{1}H NMR spectra of the complex are shown at various pHs at 5 °C. The signal at $\delta = 19$ ppm is assigned as the LBHB bridging His and Asp in the diad His 57-Asp 102. The signal at $\delta = 15$ ppm that grows in at high pHs at the expense of the 19 ppm signal is that of the unprotonated diad in free chymotrypsin. The inset is the plot of integrated intensity of the LBHB signal (I_{LBHB}) vs pH. The data do not fit equations for one- or two-proton ionization, but are fitted to the equation $I_{LBHB} = c/(1 + K/[H^+]^{1.2})$. The explanation for the partial ionization of a second proton is given in the text.

versus pH and showed a cooperative, two-proton ionization whenever the P_1 residue was phenylalanine. The data were fitted to the following equation:

$$I_{LBHB} = [\text{peptidyl-TFK}_o]/([E_o] + K/[H^+]^2)$$

where [peptidyl-TFK_o] and [E_o] refer to the total concentrations of inhibitor and chymotrypsin, respectively, and I_{LBHB} is the fraction of chymotrypsin in the form of the peptidyl-TFK−hemiketal complex. The molecular basis for the two-proton ionization is explained by eqs 2−8 of the Discussion and in an earlier article (*5*). Briefly, dissociation of the proton from $N^{\epsilon 2}$ is accompanied by the release of the peptidyl-TFK from the enzyme, hydration of the free peptidyl-TFK, and ionization of the hydrate, the pK_a of which is 9.5 (*1*, *3*).

*Interaction of N-Ac**LV**-CF_3 with Chymotrypsin.* The reaction of *N*-Ac**LV**-CF_3 with chymotrypsin also produced a tetrahedral complex with a low-field ^{1}H NMR signal of 18.9 ppm. *N*-Ac**LV**-CF_3 is a poor inhibitor ($K_i = 170$ μM) compared with any peptidyl-TFK with phenylalanine in the P_1 position; however, the low-field proton resonates at nearly the same field as the low-field proton of the complex with *N*-Ac**LF**-CF_3.

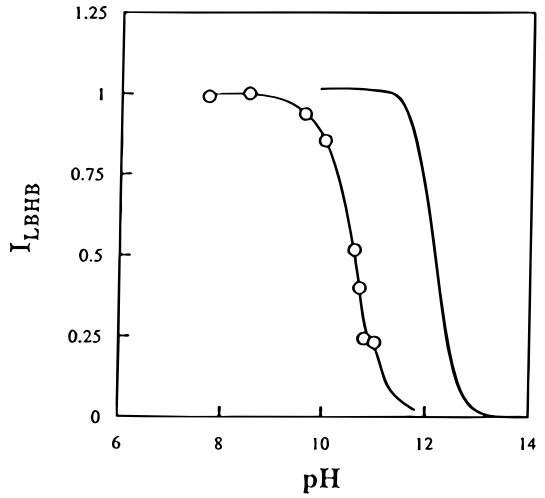

FIGURE 2: Effect of temperature on the pH titration of the *N*-Ac**LF**-CF_3−chymotrypsin complex. The titration curve previously determined at 5 °C (*5*) is shown as the solid line and corresponds to the ionization of two protons with an apparent pK_a of 12. The data shown with the open circles were obtained at 25 °C as described in Experimental Procedures. These data could not be fitted to equations for either one- or two-proton ionization, but they were fitted as shown to the equation $I_{LBHB} = c/(1 + K/[H^+]^{1.3})$. From this fitting procedure, an apparent pK_a of 10.6 was determined.

Representative NMR spectra of the downfield region and the titration curve for the fractional intensity of the low-field signal versus pH are shown in Figure 1. Although the titration curve did not describe a one-proton ionization, the data could not be fitted to an equation for a two-proton dissociation. The data were fitted to the equation $I_{LBHB} = c/(1 + K/[H^+]^{1.2})$, giving an apparent p$K_a$ value of 10.3.

The pK_a for ionization of hydrated *N*-Ac**LV**-CF_3 was 10.4 at room temperature and >11 at 5 °C. At pH 10.3 and 5 °C, about 16.6% of the hydrate was found to be ionized so that the hydrate was partially ionized throughout the pH range of the titration. As explained in the Discussion, partial ionization of the free peptidyl-TFK hydrate in the pH range of Figure 1 accounts for the observation of the less than two-proton ionization.

*Effect of Temperature on the Interaction of N-Ac**LF**-CF_3 with Chymotrypsin.* Shown in Figure 2 are the titration curves resulting from the ^{1}H NMR analysis of the downfield protons in the tetrahedral adduct of Ser 195 with *N*-Ac**LF**-CF_3 as a function of pH at 25 and 5 °C. The low-field signal is narrower at 25 °C (166 Hz, pH 7) than at 5 °C (224 Hz, pH 7), and the data at 25 °C cannot be fitted to a two-proton dissociation equation. Fitting of the titration data to the equation $I_{LBHB} = c/(1 + K/[H^+]^{1.3})$ gives an apparent pK_a value of 10.6.

Mechanistic Role of the LBHB. These results support the LBHB-facilitated general base-catalyzed mechanism of chymotrypsin action (*4*, *5*). This mechanism is illustrated in Scheme 1. The binding of substrate or a structurally related inhibitor induces a conformational change upon formation of the Michaelis complex **1**, with the introduction of steric compression between His 57 and Asp 102. Because the pK_as of Asp 102 and protonated His 57 can be similar and would

Scheme 1

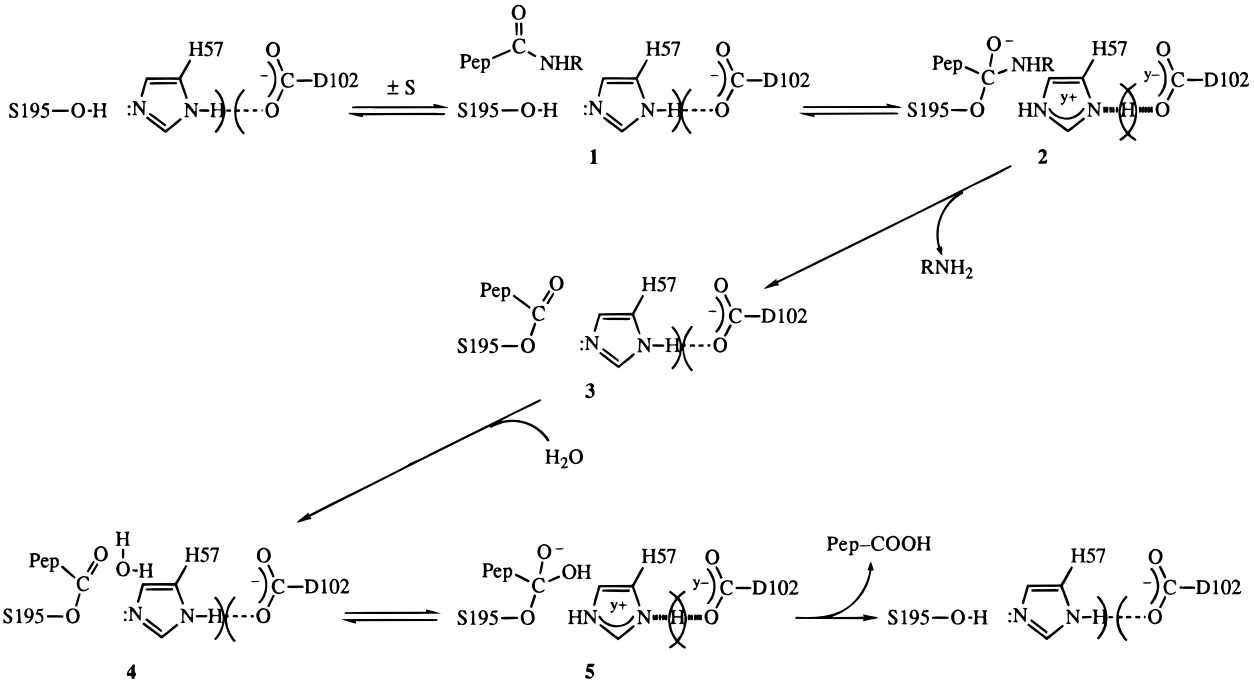

relieve the strain through the formation of a LBHB, protonation of His 57 is favored by steric compression. In this way, the basicity of $N^{\epsilon 2}$ in the His 57-Asp 102 diad is increased by substrate binding. The elevated basicity of His 57 increases its effectiveness as a base in the abstraction of a proton from Ser 195, which is required for the nucleophilic reactivity of serine in the second step to generate complex **2**, the tetrahedral intermediate or transition state.[3] Elimination of the leaving group from **2** requires proton transfer from His 57 to RNH_2 to form complex **3**, the acyl−enzyme intermediate. Hydrolysis of **3** follows the analogous course through complexes **4** and **5**, in which H_2O acts in place of the leaving group RNH_2 and accepts the acyl group from Ser 195.

The reaction of peptidyl-TFKs with chymotrypsin follows the first two steps of the overall hydrolysis mechanism to form the peptidyl-TFK analogue of the tetrahedral intermediate or transition state. A peptidyl-TFK complex (structure A) is compared with intermediate **2** (structure B) below.

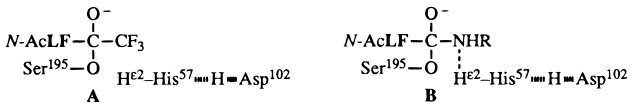

The nucleophilic addition of Ser 195 to the peptidyl group is the most difficult process in the hydrolysis of a peptide bond. Therefore, the reactions of peptidyl-TFKs with chymotrypsin are pertinent to the hydrolytic mechanism. We have examined the effects of varying the aminoacyl residues of peptidyl-TFKs on the basicities of His 57-$N^{\epsilon 2}$ in the trifluoromethyl analogues of complex **2**.

Cooperative Ionization of His 57-$N^{\epsilon 2}$ in Complexes of Peptidyl-TFKs with Chymotrypsin. The ionization of His 57 in peptidyl-TFK complexes with chymotrypsin appears to be coupled with the dissociation of the inhibitor from the active site (*5*). Evidence for this is provided by the fact that ionization of His 57 is associated with the disappearance of the very low-field proton NMR signal ranging from 18.5 to 19.1 ppm, depending on the structure of the peptidyl group, and the appearance of the 15.0 ppm signal characteristic of free chymotrypsin at high pH. Both the field position and the signal width of the 15 ppm species are indistinguishable from those for free chymotrypsin, and both parameters are independent of the peptidyl-TFK. Dissociation of the inhibitor (eq 3) touches off the processes described by eqs 4−8.

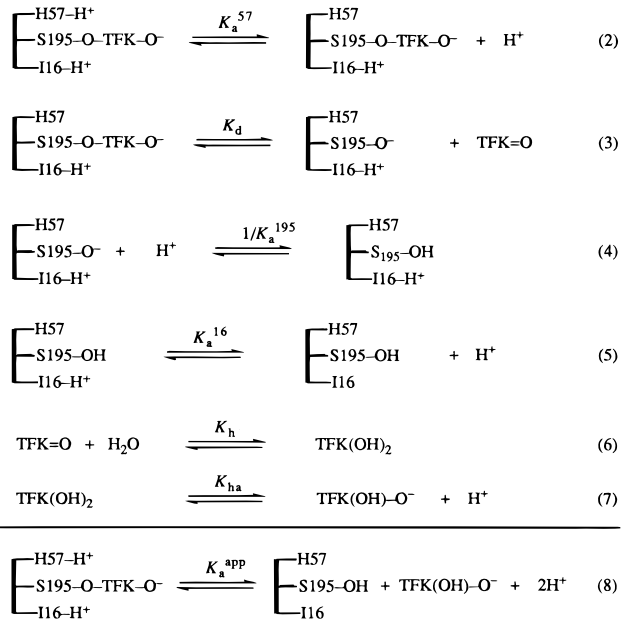

[3] The hydrolysis of substrates with excellent leaving groups such as *p*-nitrophenolate ion does not necessarily involve the formation of a discrete tetrahedral intermediate. An extensive set of kinetic isotope effects on the hydrolysis of *p*-nitrophenyl acetate by chymotrypsin, carbonic anhydrase, papain, and *Aspergillus* acid protease shows that hydrolysis proceeds by a concerted process through a tetrahedral-like transition state, in which no discrete tetrahedral intermediate is formed (R. A. Hess, A. C. Hennge, and W. W. Cleland, submitted for publication).

These are cascading steps that include the protonation of Ser 195, the ionization of Ile 16, the hydration of the keto form of the peptidyl-TFK, and the ionization of the peptidyl-TFK hydrate. The acid dissociation constants of His 57, Ser 195, Ile 16, and the peptidyl-TFK hydrate are K^{57}, K^{195}, K^{16}, and K_{ha}, respectively; the dissociation constant for the peptidyl-TFK from the unprotonated diad His 57-Asp 102 is K_d, and the hydration constant for the peptidyl-TFK is K_h. The overall process releases two protons upon ionization of His 57 when the equilibria of eqs 3−7 all lie far to the right. Because $pK^{195} \approx 14$ (*16*), $pK^{16} = 8.2$ (*17*, *18*), $pK_{ha} = 9.5$, and $K_h = 4500$ (for *N*-Ac**LF**-CF_3) (*1*−*3*), ionization with release of two protons can be observed if the pK_a of His 57 is between 10 and 12 and the value of K_d is large. Under these conditions, it can be shown that the fraction of enzyme in the form of the low-barrier hydrogen-bonded complex (I_{LBHB}) is given by eq 9.

$$I_{LBHB} = \frac{[TFK_o]}{[E_o] + K_a^{app}/[H^+]^2} \quad (9)$$

Here, the total concentrations of peptidyl-TFK and enzyme are $[TFK_o]$ and $[E_o]$, respectively, and neither is present in large excess over the other. Data for the ionizations of hemiketal complexes of chymotrypsin with *N*-Ac**LF**-CF_3, *N*-Ac**F**-CF_3, *N*-Ac**VF**-CF_3, and *N*-Ac**GF**-CF_3 at 5 °C are well fitted by eq 9. In these cases, the value of pK_a^{app} can be regarded as a good estimate of pK^{57}.

Data for *N*-Ac**LV**-CF_3 at 5 °C in Figure 1 cannot be fitted to eq 9 but can be fitted to a similar equation in which the exponent for $[H^+]$ is 1.2. The release of less than two protons presumably means that one of the conditions for the validity of eq 9 is not met by this inhibitor. The value of pK_{ha} is ≥11 for *N*-Ac**LV**-CF_3 at 5 °C. Therefore, ionization of the peptidyl-TFK hydrate (eq 7) will partially limit the overall ionization process in this case, which accounts for decreased cooperativity in proton release. The higher value of pK_{ha} (≥11) for *N*-Ac**LV**-CF_3 relative to that for *N*-Ac**LF**-CF_3 (9.5) can be rationalized by the effects of branching at C3 of valyl-TFK, which can decrease the polarity in the vicinity of the hydrate and destabilize the anionic ionized form. Although the hydration constant (eq 6) for *N*-Ac**LV**-CF_3 has not been measured, side chain branching in valyl-TFK can be expected to decrease it, and this too would tend to limit the observed proton release.

A conventional interpretation of cooperative ionization curves at high pHs is that the protein is undergoing denaturation, with consequent multiple ionizations. Four facts fail to support a simple denaturation model at pH 10−12. First, the changes in low-field NMR signals are time-independent (*5*), so any denaturation must be reversible. Second, the interaction between His 57 and Asp 102 is observed ($\delta = 15$ ppm) in the ionized form, so the active site structure is retained. Third, the processes of eqs 2−7 must take place in any case, and they mandate the observed cooperative ionization. Proton release owing to denaturation would have to contribute ionizations in addition to those in eqs 2−7, and none are observed. Fourth, a denaturation model would require highly cooperative ionization behavior for all inhibitors, especially poor inhibitors. On the contrary, the chymotrypsin complex with the poor inhibitor *N*-Ac**LV**-CF_3 undergoes only a slightly cooperative proton release ($[H^+]^{1.2}$), and this is consistent with eqs 2−7 in the light of the fact that $K_{ha} \geq 11$ for *N*-Ac**LV**-CF_3.

The ionization data for the tetrahedral complex of chymotrypsin with *N*-Ac**LF**-CF_3 at 25 °C also do not fit eq 9 (Figure 2), although the fit is good at 5 °C (*5*). At 25 °C, the titration data are fitted with 1.3 being the exponent of $[H^+]$. Presumably, one or more of the equilibria of eqs 3−7 are sufficiently temperature sensitive to cause this effect, which also decreases the value of pK_a^{app} from 12.0 to 10.6. The known values of K_h and K_{ha} for this inhibitor at 25 °C are 4500 and 3×10^{-10}, respectively (*1*−*3*), so that eqs 6 and 7 should be far to the right in the range of pH 10−12. Similarly, the values of pK^{16} and pK^{195} at 25 °C should prevent eqs 4 and 5 from controlling the ionization. Perhaps eq 3 becomes a controlling factor at 25 °C. This binding step is postulated to include an enzyme conformational change (*5*) which may be temperature sensitive. In any case, pK_a^{app} is a minimum estimate for pK^{57}. At 5 °C, the ionization behaves according to eq 9, and the value of pK_a^{app} (12.1) is probably close to that of pK^{57}. At higher temperatures, the ionization is less highly cooperative and the value of pK_a^{app} (10.6) is less than that of pK^{57}, which is probably between 11 and 12.

Consequences of Varying the P_1 Residue. Variations in the P_1 residue unpredictably affect the apparent basicity of His 57 in the hemiketal adduct. Changing the phenylalanyl residue to naphthyl (*N*-Ac**LNp**-CF_3) decreases pK_a^{app} to 10.9, and valine in this position (*N*-Ac**LV**-CF_3) leads to a pK_a^{app} of 10.3. *N*-Ac**LNp**-CF_3 is a very potent inhibitor ($K_i < 1$ μM), but *N*-Ac**LV**-CF_3 is a weak inhibitor ($K_i = 170$ μM). Variation of the P_1 residue in peptidyl-TFKs can be expected to affect the hydration equilibria and the pK_as of the peptidyl-TFK hydrates in ways that are difficult to predict. These properties contribute to the overall ionization of chymotrypsin−peptidyl-TFK adducts. Because of the complexities of the binding process for the largely hydrated peptidyl-TFKs, it is difficult to rationalize the consequences of altering the P_1 residue.

Importance of the P_2 Residue to the Basicity of His 57, Inhibition by Peptidyl-TFKs, and Activity of Chymotrypsin. The results from varying the P_2 residues in peptidyl-TFKs, while keeping P_1 phenylalanyl, reveal interesting correlations of K_i, pK^{57}, and δ_{LBHB}, as well as k_{cat}/K_m for the corresponding peptidyl methyl ester substrates. Shown in Figure 3A is the linear correlation of log K_i with pK^{57} of the hemiketal adducts, in which the slope is −0.77. Shown in Figure 3B is a plot of log k_{cat}/K_m for analogous peptidyl methyl esters acting as substrates versus the apparent pK^{57} for the peptidyl-TFKs acting as inhibitors. The points define a line with a slope of 0.68. The positive correlation of pK_a with log k_{cat}/K_m is evidence of the importance of the basicity of His 57 to catalysis. Limited data are available for the parameters in Figure 3, and the observation of straight lines does not necessarily mean that proportionality would hold over a much larger range of values.

Data points for *N*-Ac**LV**-CF_3 and *N*-Ac**LV**-OCH_3 lie above the line in the plot of log K_i (Figure 3A) and below the line in the plot of log k_{cat}/K_m (Figure 3B), confirming the importance of the P_1 residue to inhibition and enzymatic activity. A complete analysis of the consequences of varying the P_1 residue is not possible owing to insufficient data.

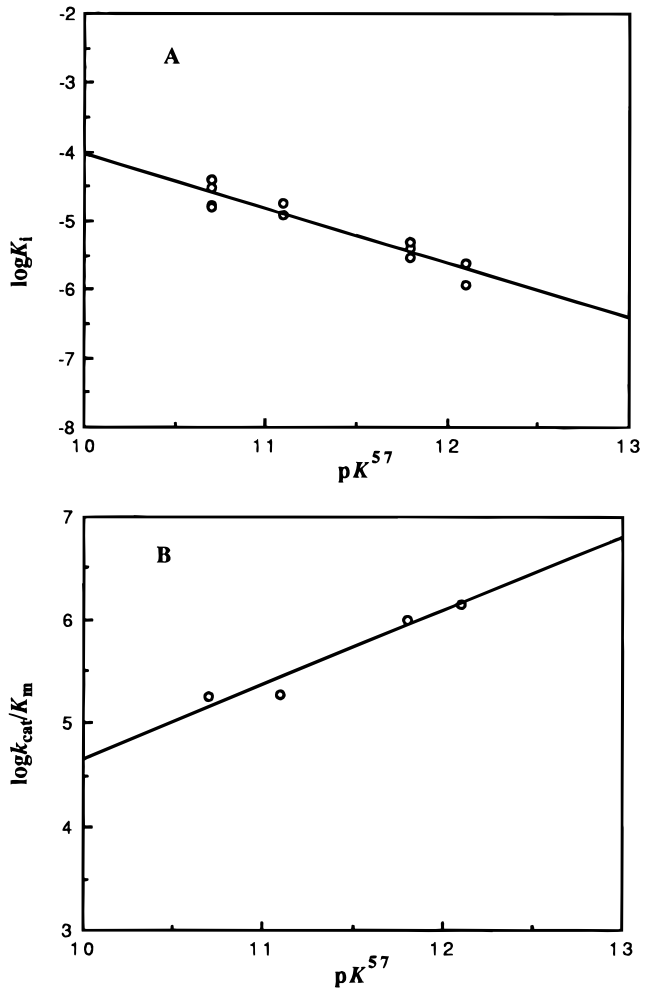

FIGURE 3: Linear free energy correlations for peptidyl-TFK−chymotrypsin complexes. Literature values (*1*, *2*) of log K_i for peptidyl-TFKs (A) acting as inhibitors of chymotrypsin and log k_{cat}/K_m for corresponding peptidyl methyl ester substrates (B) are plotted vs pK^{57} (this work) in the peptidyl-TFK−chymotrypsin complexes. Values of pK^{57} are taken as pK_a^{app} in eq 9 for complexes that undergo two-proton ionizations (see the text). In the peptidyl-TFKs and methyl esters, the P_1 position is occupied by phenylalanine, and the P_2 position is *N*-Ac, *N*-Ac-Gly, *N*-Ac-Val, or *N*-Ac-Leu. The slope of the line for log K_i is −0.77 (A), and that for log k_{cat}/K_m (B) is 0.68.

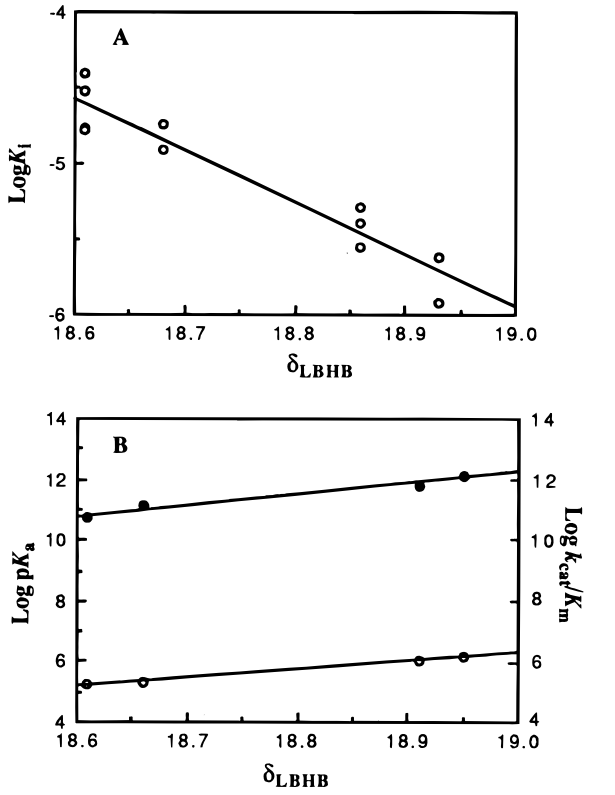

FIGURE 4: Correlations of δ_{LBHB} for chymotrypsin−peptidyl-TFK complexes. (A) Values of log K_i for inhibition of chymotrypsin by peptidyl-TFKs are plotted vs δ_{LBHB} for the peptidyl-TFK complex to give a slope of −3.0. (B) Values of pK^{57} for His 57 in chymotrypsin−peptidyl-TFK complexes are plotted (●) vs δ_{LBHB} to give a slope of 3.7. Values of log K_{cat}/K_m for methyl esters analogous to the peptidyl-TFK complexes are plotted (○) vs δ_{LBHB} to give a slope of 2.7. Data for peptidyl groups with Phe in the P_1 position and *N*-Ac, *N*-AcGly, *N*-Ac-L-Val, or *N*-Ac-L-Leu in P_2 are taken from Table 1.

The relationships of the chemical shift of the LBHB proton in the chymotrypsin−peptidyl-TFK adducts to pK^{57}, to log K_{cat}/K_m for analogous peptidyl methyl esters, and to K_i for inhibition are depicted in Figure 4. The slopes of the lines are −3.5 ppm^{-1} for log K_i versus δ_{LBHB} in Figure 4A. In Figure 4B, the slopes are 3.7 ppm^{-1} for pK^{57} versus δ_{LBHB} and 2.7 ppm^{-1} for log k_{cat}/K_m versus δ_{LBHB}. These refer to L-Phe in the P_1 position and *N*-Ac, *N*-AcGly, *N*-Ac-L-Val, or *N*-Ac-L-Leu in the P_2 position. The leucyl residue is the best P_2 residue with respect to the value of K_i in this series (*2*), and it also gives the lowest-field chemical shift, the highest pK^{57}, and the highest value of k_{cat}/K_m. The correlations break down with changes in the residue at P_1, as does the published correlation between log K_i and log k_{cat}/K_m for these inhibitors (*2*).

The value of δ_{LBHB} in simple compounds increases with decreasing interatomic distance separating heteroatoms engaged in hydrogen bonding (*13*). The length of a hydrogen-bonded contact is also correlated with its strength. For example, the closer the O−O contact in the formate···formic acid hydrogen bond, the stronger the bond (*14*). The values of 18−19 ppm for δ_{LBHB} in chymotrypsin−peptidyl-TFKs are clearly in the range for LBHBs (*4*, *15*), and they increase with increasing inhibitory potency and increasing reactivity of the corresponding substrates. The lines in Figure 4 indicate that increasing pK^{57} and substrate reactivity are correlated with decreasing length and increasing strength of the LBHB. Independent, X-ray crystallographic measurements of the separations between His 57-N$^{\delta 1}$ and Asp 102-O$^{\delta 1}$ in the hemiketal complexes of chymotrypsin with *N*-Ac**LF**-CF_3 (2.5 Å) and *N*-Ac**F**-CF_3 (2.6 Å) support these conclusions (*16*).

*Temperature Effects on the Properties of the Hemiketal Analogues of the Tetrahedral Intermediate **2**.* The NMR signal for the low-field proton in free chymotrypsin at low pH is best observed at low temperatures, presumably because it is in chemical exchange with water protons at a rate that is too fast to allow it to be observed on the NMR time scale at room temperature. For this reason, the LBHB in protonated chymotrypsin is normally observed at 3−5 °C (*4*, *9*, *17*, *18*). However, the low-field proton in the hemiketal adduct of chymotrypsin with *N*-Ac**LF**-CF_3 is readily observable at 25 °C. The signal is narrower at 25 °C than at 5 °C, presumably due to the increased tumbling rate of the protein. Inasmuch as the NMR signal for the LBHB is observed at 25 °C, its rate of chemical exchange with water protons must

be slower than that of the LBHB proton in free protonated chymotrypsin. The difference in exchange rates may be due to a difference in the conformational equilibria between free chymotrypsin and the tetrahedral hemiketal complexes. The chymotrypsin−peptidyl-TFKs complexes are likely to be less conformationally mobile than the free enzyme. If conformational flexibility contributes to the exchange rate, the peptidyl-TFK complexes, which are transition state analogues, will undergo chemical exchange at a slower rate than the free enzyme. Alternatively, the bridging proton may simply be more tightly bonded in the case of the peptidyl-TFK complexes than in free chymotrypsin at low pH.

Extent of Proton Transfer in Hemiketal Adducts of Peptidyl-TFKs with Serine Proteases. Ash et al. (*19*) presented a skeptical view of LBHBs in serine proteases. Their NMR experiments on a peptidyl−boronate complex of α-lytic protease indicated the absence of a LBHB. Peptidyl−boronate complexes of serine proteases differ electrostatically from transition states in that the negative charge is formally localized on boron and not on the oxygen in the anion binding site. Moreover, the oxyanion binding site is occupied by a hydroxyl group, and the distance between His 57 and Asp 102 is too long for a LBHB (*20*). A peptidyl-TFK adduct seems similar to the transition state and is compared below with a peptidyl−boronate adduct to illustrate the differences.

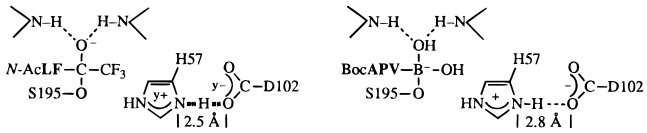

The spacings between His 57 and Asp 102 refer to the chymotrypsin adduct of *N*-Ac**LF**-CF_3 (*16*) and the α-lytic protease adduct of Boc**APV**B$(OH)_2$ (*20*). The chemical shifts for protons bridging His 57 and Asp 102 in peptidyl−boronate complexes are typically 16−17 ppm (*19*), whereas they are 18.6−19.0 for peptidyl-TFK complexes. The spacing between His 57 and Asp 102 in the peptidyl−boronate complex and the coupling constant $^1J_{NH}$ for $N^{\delta 1}$ are consistent with a conventional ionic interaction.

In the case of the *N*-Ac**LF**-CF_3 adduct with chymotrypsin, the spacing between His 57 and Asp 102 and the low-field ^{1}H NMR signal are consistent with a LBHB. The interaction has been formulated as ionic but with depolarization of charges as y^+ on His 57 and y^- on Asp 102, such that $0.5 \leq y < 1.0$ (*4*). A symmetrical hydrogen bond corresponds to $y = 0.5$, and an unsymmetrical low-barrier hydrogen bond corresponds to $0.5 < y < 1.0$. Halkides et al. (*21*) have estimated from the ^{15}N NMR chemical shifts of His 57 that the LBHB proton is 30% transferred in a peptidyl-TFK complex of subtilisin, in which the low-field proton appears at 18.8 ppm. Thirty percent transfer corresponds to $y = 0.7$ in the LBHB complex. Another estimate can be made from the coupling constant $^1J_{NH}$ value of 81 Hz reported by Halkides et al. for the same complex. Correlation with the $^1J_{NH}$ coupling constants in an extensive series of pyridinium salts of carboxylic acids (*22*) indicates about 20% proton transfer, corresponding to $y = 0.8$ in the LBHB complex. Both estimates indicate substantial proton transfer in the hemiketal complexes of peptidyl-TFKs with serine proteases. To the extent that they resemble the transition state, they represent the degree of proton transfer within the LBHB in the transition state.

The similarity of peptidyl-TFK adducts of chymotrypsin to the transition state is supported by the dissociation constant K_d for *N*-Ac**LF**-CF_3. The inhibition constant K_i is 1×10^{-6} M, and this refers to the peptidyl-TFK in aqueous solution, where it exists as its hydrate. Because only the keto form reacts with the enzyme, the dissociation constant refers to the reaction of the keto form. The hydration constant K_h for *N*-Ac**LF**-CF_3 has been measured (*2*) and was found to be 4.5×10^3. The dissociation constant is given by $K_d = K_i/K_h$, and by this calculation, $K_d = 2 \times 10^{-10}$ M (*2*), which represents very tight binding of *N*-Ac**LF**-CF_3.

Peptide boronic acids are also very tightly bound; however, the binding of boronic acids is augmented by the strength of the B−O bond. The strength of a covalent bond is related to the electronegativity difference between the participating atoms, the strongest bonds being between atoms differing the most in electronegativity (*23*). From tabulated values of the strengths of covalent bonds, one can estimate by interpolation that the B−O bond can be expected to be stronger than the C−O bond by about 10 kcal mol^{-1}, on the basis of the Pauling electronegativity difference of 1.4 between boron and oxygen compared with the difference of 1.0 between carbon and oxygen (*23*). This expectation is supported by data on the bond dissociation energy of a C−O bond in an ether of 80 kcal mol^{-1} (*24*) and the bond dissociation energy of 93 kcal mol^{-1} for the MeO−B bond in a boric acid triester (*25*). Bond dissociaton energies for perfect analogues of the hemiketal adducts of peptidyl-TFKs and boronate adducts of peptide boronic acids are not available; however, all literature on the strengths of covalent bonds indicates that B−O bonds are stronger than C−O bonds. Therefore, the intrinsic strength of the B−O bond will augment the binding of peptide boronic acids to Ser 195 irrespective of any similarities between the boronate adduct and the transition state for peptide hydrolysis. For this reason, direct comparisons of the dissociation constants for the peptidyl-TFKs and the peptide boronic acids do not bear on their relative similarities to the transition state. Comparisons within groups of the two types of inhibitors, as in plots of log k_{cat}/K_m versus log K_d for a series of peptide boronic acids or peptidyl-TFKs, are appropriate for determining the contributions of the peptidyl groups in overall binding.

Summary of the Evidence Supporting the Mechanism of Scheme 1. The novel aspects of the mechanism in Scheme 1 are the LBHB in the tetrahedral intermediates **2** and **5** and the steric compression in the Michaelis complexes **1** and **4** and the acyl−enzyme intermediate **3**. Evidence for the LBHB includes the low-field chemical shift of the protonated diad, particularly in the peptidyl-TFK complexes (*3*−*5*, *17*, *18*), the close spacing between His 57 and Asp 102 in the *N*-Ac**LF**-CF_3 and *N*-Ac**L**-CF_3 complexes (*16*), the deuterium isotope effect on the chemical shift of the low-field proton in the *N*-Ac**LF**-CF_3 complex (*26*), the low fractionation factor for the low-field proton in the *N*-Ac**LF**-CF_3 complex,[4] and the low fractionation factors for the low-field protons in

[4] J. Lin, W. M. Westler, J. L. Markley, and P. A. Frey, research in progress.

[5] M. J. Cloninger and P. A. Frey, submitted for publication.

analogous complexes of subtilisin and chymotrypsinogen (*21*, *27*).

Little direct evidence supporting compression between His 57 and Asp 102 in Michaelis complexes such as **1** and **4** is available owing to the many difficulties associated with studies of reacting systems. However, the acyl−enzyme intermediate **3** includes the acyl group interactions at sites P_1, P_2, etc., and is related in this way to Michaelis complexes. Two high-resolution structures (1.8 Å) of γ-chymotrypsin, one at low pH and the other at high pH, have shown that it is an acyl−enzyme intermediate and may be regarded as a species of complex **3** in Scheme 1. In both structures, the distance between $N^{\delta 1}$ of His 57 and $O^{\delta 1}$ of Asp 102 is 2.64 Å (*28*, *29*). This distance supports the postulated compression in Scheme 1. While the modeled spacing of 2.64 Å cannot prove compression, owing to the uncertainty of ±0.2 Å even in a high-resolution structure, a modeled distance of 2.8−2.9 Å that is conventionally observed for hydrogen bonded N−O contacts would rule out compression. The conventional distance was not observed, and the close contact supports the postulated compression.

Steric Compression and Perturbations in Acid−Base Strength in Related Systems. The possible roles of LBHBs in enzymatic reactions have been discussed (*30*). According to Scheme 1, steric compression between His 57 and Asp 102 of serine proteases is induced by substrate binding and increases the basicity of His 57 through LBHB formation upon protonation. Support for this concept is provided by steric enhancement of imidazole basicity in derivatives of *cis*-urocanic acid.[5] Spectroscopic and crystallographic work on Δ^5-3-ketosteroid isomerase has led to a similar proposal for the role of a LBHB between Asp 99 and Tyr 14 in the reaction mechanism (*31*, *32*).

REFERENCES

1. Imperiali, B., and Abeles, R. H. (1986) *Biochemistry 25*, 3760−3767.
2. Brady, K., and Abeles, R. H. (1990) *Biochemistry 29*, 7608−7617.
3. Liang, T.-C., and Abeles, R. H. (1987) *Biochemistry 26*, 7603−7608.
4. Frey, P. A., Whitt, S. A., and Tobin, J. B. (1994) *Science 264*, 1927−1930.
5. Cassidy, C. S., Lin, J. L., and Frey, P. A. (1997) *Biochemistry 36*, 4576−4584.
6. Kraut, J. (1971) *Annu. Rev. Biochem. 46*, 331−358.
7. Bergeson, S. H., Edwards, P. D., Shweartz, J. A., Shaw, A., Square, K., Stein, M. M., Trainor, D. A., Mills, G., Wildonger, R. A., and Wolanin, D. J. (1990) U.S. Patent 4,910,190.
8. Hore, P. J. (1983) *J. Magn. Reson. 55*, 283−300.
9. Zhong, S., Haghjoo, K., Kettner, C., and Jordan, F. (1995) *J. Am. Chem. Soc. 117*, 7048−7055.
10. Bruice, T. C., Fife, T. H., Bruno, J. J., and Brandon, N. E. (1962) *Biochemistry 1*, 7−12.
11. Himoe, A., Parks, P. C., and Hess, G. P. (1967) *J. Biol. Chem. 242*, 919−929.
12. Fersht, A. R., and Requena, Y. (1971) *J. Mol. Biol. 60*, 279−290.
13. McDermott, A., and Ridenour, C. F. (1996) in *Encyclopedia of NMR*, pp 3820−3824, Wiley and Sons, Ltd., Sussex, England.
14. Pan, Y., and McAllister, M. A. (1997) *J. Am. Chem. Soc. 119*, 7561−7566.
15. Hibbert, F., and Emsley, J. (1990) *Adv. Phys. Org. Chem. 26*, 255−379.
16. Brady, K., Wei, A., Ringe, D., and Abeles, R. H. (1990) *Biochemistry 29*, 7600−7607.
17. Robillard, G., and Shulman, R. G. (1974) *J. Mol. Biol. 86*, 519−540.
18. Markley, J. L. (1978) *Biochemistry 17*, 4648−4656.
19. Ash, E. L., Sudmeier, J. L., DeFabo, E. C., and Bachovchin, W. W. (1997) *Science 278*, 1128−1131.
20. Bone, R., Shenvi, A. B., Kettner, C. A., and Agard, D. A. (1987) *Biochemistry 26*, 7609−7614.
21. Halkides, C. J., Wu, Y. Q., and Murray, C. J. (1996) *Biochemistry 35*, 15941−15948.
22. Smirnov, S. N., Golubev, N. S., Denisov, G. S., Benedict, H., Schah-Mohammedi, P., and Limbach, H.-H. (1996) *J. Am. Chem. Soc. 118*, 4094−4101.
23. Cotton, F. A., and Wilkinson, G. (1962) *Advanced Inorganic Chemistry*, pp 85−95, Wiley and Sons, New York.
24. Kerr, J. A. (1966) *Chem. Rev. 66*, 465−500.
25. Pilcher, G., and Skinner, H. A. (1982) in *The Chemistry of the Metal−Carbon Bond* (Hartley, F. R., and Patai, S., Eds.) Chapter 2, pp 43−90, Wiley and Sons, New York.
26. Cassidy, C. S. (1997) Ph.D. Dissertation, University of Wisconsin−Madison, Madison, WI.
27. Markley, J. L., and Westler, W. M. (1996) *Biochemistry 35*, 11092−11097.
28. Dixon, M. M., Brennan, R. G., and Matthews, B. W. (1991) *Int. J. Biol. Macromol. 13*, 89−96.
29. Dixon, M. M., and Matthews, B. W. (1989) *Biochemistry 28*, 7033−7038.
30. Gerlt, J. A., Kreevoy, M. M., Cleland, W. W., and Frey, P. A. (1997) *Chem. Biol. 4*, 259−267.
31. Zhao, Q., Abeygunawardana, C., Gittis, A. G., and Mildvan, A. S. (1997) *Biochemistry 36*, 14616−14626.
32. Kim, S. W., Cha, S.-S., Cho, H.-S., Kim, J.-S., Ha, N.-C., Cho, M.-J., Joo, S., Kim, K. K., Choi, K. Y., and Oh, B.-H. (1997) *Biochemistry 36*, 14030−14036.

BI980278S